age through the refrigeration clamps, the absolute concentration measurements for the TT-014 samples are accurate to only about 1 to 2%. The mass spectrometer system employed a low-temperature (40°K) charcoal trap to separate helium from neon before analysis.
16. M. Kodera, G. Igarashi, M. Ozima, *Earth Planet. Sci. Lett.* **87**, 266 (1988).
17. Potential density is the density of seawater ρ corrected for adiabatic effects by the use of potential temperature θ instead of in situ temperature *T*. θ is the temperature of a parcel of water that has been brought adiabatically to the ocean surface without thermal contact with the surrounding ocean. In oceanography, density is usually expressed as the density anomaly $\sigma = (\rho - 1) \times 10^3$. Thus, a potential density of $\sigma_\theta = 27.3$ corresponds to $\rho_\theta = 1.0273$ g cm^{-3}.
18. E. T. Baker, R. A. Feely, M. J. Mottl, J. E. Lupton, *ibid.* **128**, 1 (1994).
19. J. L. Reid, in *Evolution of Physical Oceanography*, B. A. Warren and C. Wunsch, Eds. (MIT Press, Cambridge, MA, 1981), pp. 70–111.
20. V. A. Burkov, R. P. Bulatov, V. G. Neiman, *Oceanology* **13**, 325 (1973).
21. L. Talley, personal communication.
22. K. Yoshida and T. Kidokoro, *J. Oceanogr. Soc. Jpn.* **23**, 88 (1967); *ibid.*, p. 231.
23. J. L. Reid and A. W. Mantyla, *J. Phys. Oceanogr.* **8**, 946 (1978).
24. W. Jenkins, personal communication.
25. J. G. Moore and W. W. Chadwick Jr., in *Mauna Loa: A Decade Volcano*, J. M. Rhodes and J. P. Lockwood, Eds. (Geophysical Monograph Series, American Geophysical Union, Washington, DC, in press).
26. I thank K. Roupe, R. Greene, G. Paradis, G. Lebon, C. Massey, and M. Landsteiner for assistance with sample collections at sea; L. Evans, R. Greene, R. Kovar, and G. Paradis for the shore-based sample processing and helium isotope measurements; A. Bobbitt for assistance with the figures; L. Talley, D. Roemmich, J. Swift, J. Bullister, G. Johnson, and G. Cannon, who served as chief scientists on the expeditions involved and provided strong support for the helium work; W. Jenkins for making his WOCE P4 and P16 data available before publication; and L. Talley, J. Reid, and W. Jenkins for helpful discussions. Supported by the NOAA VENTS Program and by grants OCE91-05884 and OCE92-96169 from the Ocean Sciences Division of NSF. This is PMEL contribution number 1698.

21 November 1995; accepted 4 March 1996

Selected Elastic Moduli of Single-Crystal Olivines from Ultrasonic Experiments to Mantle Pressures

Ganglin Chen,* Baosheng Li, Robert C. Liebermann

Ultrasonic interferometric measurements, developed for polycrystalline samples in a multi-anvil apparatus, were extended to single-crystal samples of San Carlos olivine and forsterite. The elastic moduli, C_{22} and C_{55} of San Carlos olivine and C_{55} of pure forsterite, were measured to about 13 gigapascals. These data on C_{22} for San Carlos olivine and C_{55} for forsterite are consistent with earlier measurements and extrapolations. The C_{55} for San Carlos olivine increases linearly as a function of increasing pressure, unlike the earlier nonlinear behavior observed at high pressure with impulsive stimulated scattering techniques.

Understanding the dynamics of Earth's mantle depends critically on the models of its mineralogical and chemical composition as a function of depth. Direct information on the composition comes from comparison of seismic profiles of the mantle with the sound velocities of candidate minerals measured in the laboratory. Olivine $[(Mg,Fe)_2SiO_4]$ is one of the major constituents of the upper mantle; this mineral transforms to a β phase (wadsleyite) and a spinal polymorph (ringwoodite) at the pressures and temperatures of the mantle transition zone (410 to 660 km). The significance of the sound velocities of olivine and its high-pressure polymorphs in the interpretation of the mantle composition has motivated measurements on this mineral to successively higher pressures. The earliest ultrasonic measurements were limited to pressures below 1 GPa (*1*, *2*). These low-pressure data for olivine have been used to construct mantle mineralogical models (*3*). Webb (*4*) measured the sound velocities of single crystals of San Carlos olivine $[(Mg_{0.9}Fe_{0.1})_2SiO_4]$ in a liquid-medium pressure vessel to 3 GPa using ultrasonic interferometry; she observed a slightly nonlinear dependence of certain elastic moduli (C_{ij}) with pressure. Using impulsive stimulated scattering (ISS), Zaug *et al.* (*5*) measured the elastic moduli of San Carlos olivine to 12.5 GPa in a diamond-anvil cell and observed a pronounced curvature in the variation of C_{55} as a function of increasing pressure. Their data suggest that the *P*- and *S*-wave velocities of olivine at a depth of 410 km are lower than those calculated from the third-order finite strain extrapolation of low-pressure elasticity data (*3*).

Recently, Duffy *et al.* (*6*) and Zha *et al.* (*7*) measured the sound velocities of single-crystal forsterite (Mg_2SiO_4) using Brillouin spectroscopy in a diamond-anvil cell; their results exhibit good agreement with those of Yoneda and Morioka (*8*) measured to 6 GPa. Neither of these studies indicated a nonlinear behavior of C_{55} versus pressure. However, the issue of whether this curvature exists for iron-bearing olivine is unresolved because Yoneda and Morioka and Duffy *et al.* used pure forsterite crystals; no pure mode directions were measured in the latter study (*6*).

We report here the results of ultrasonic interferometric measurements on single crystals of both San Carlos olivine and pure forsterite in a multi-anvil apparatus (*9*). The goals of these experiments were (i) to test the feasibility of using this technique with single-crystal samples and (ii) to understand the behavior of the C_{55} mode of olivine under high pressure. We also report measurements for the longitudinal mode C_{22}, for which there is good agreement between the data of Webb (*4*) and those of Zaug *et al.* (*5*).

We measured the acoustic travel times through the olivine and forsterite samples by ultrasonic interferometry (*10*). To convert the travel times to elastic moduli, we used thermoelastic identities:

$$C_{ij} = C_{ij}^0(\rho/\rho_0)(L/L_0)^2(t_0/t)^2$$

where the subscript or the superscript zero denotes the value at ambient pressure. The quantity C_{ij} is the corresponding elastic modulus (ij = 22 or 55 in the present study), ρ is the density, *L* is the sample length, and *t* is the travel time. The precision in the travel time measurements is better than 0.2%, and the effect of the gold foil bond introduces uncertainties in the travel time on the order of 0.1%. Published data (*4*) were used to calculate the density

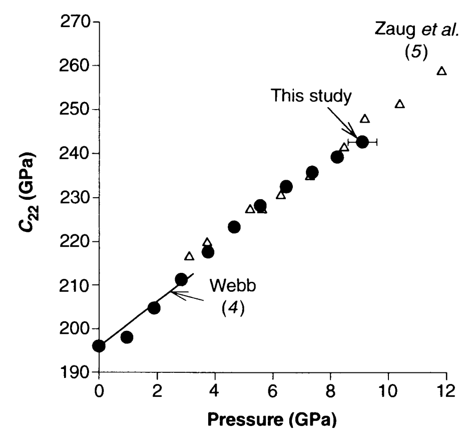

Fig. 1. Longitudinal elastic modulus C_{22} versus pressure for single crystals of San Carlos olivine. Filled circles, data from this study; solid line, data from (*4*); and triangles, data from (*5*). The uncertainties in pressures are indicated by the horizontal error bars shown for the highest pressure data points in all three figures. The uncertainties in the elastic moduli in this study are about the size of the symbol.

Center for High Pressure Research, Department of Earth and Space Sciences, State University of New York, Stony Brook, NY 11794, USA.

*To whom correspondence should be addressed.

and length changes as functions of pressure; the differences between the calculated C_{ij} based on the use of different data sets to convert our travel times to the elastic moduli are less than 0.1%. Thus, the uncertainties for the moduli are less than 0.5%.

Our ultrasonic data on C_{22} for San Carlos olivine agree at high pressures with the extrapolation of Webb's low-pressure ultrasonic data (*4*) and the ISS data of Zaug *et al.* (*5*) (Fig. 1). Our results on C_{55} for forsterite to 10 GPa agree with earlier ultrasonic results (*8*) and Brillouin spectroscopy data (*6, 7*) (Fig. 2).

We determined C_{55} as a function of increasing pressure for San Carlos olivine with one sample oriented parallel to the [100] axis and another sample oriented parallel to the [001] axis to clarify the behavior of this mode. The first experiment was made for the [001] orientation (polarization of S-wave [100]) to ~9.6 GPa (first ZnTe phase transition), and the second experiment was made for the [100] orientation (polarization [001]) to about 13 GPa (the pressure of 12.0 GPa is marked by the second ZnTe phase transition). The two experiments yielded consistent results on C_{55} for San Carlos olivine as a function of pressure and demonstrate that neither measurement was contaminated by misorientation of the transducer or the sample. At low pressure (to ~8 GPa), our results agree with (*4*) and (*5*) (Fig. 3). Above 9 GPa our results deviate from the downward curvature of C_{55} versus pressure in the measurements of (*5*). At 13.5 GPa (depth of ~410 km), our value of C_{55} is about 6% higher than that of Zaug *et al.* (*5*).

Table 1 summarizes our results on C_{55} for San Carlos olivine and forsterite, along with the results of earlier studies. Neither the Brillouin spectroscopy (*6, 7*) nor our ultrasonic data exhibit the nonlinear dependence of C_{55} on pressure observed by Zaug *et al.* (*5*); thus, shear velocities in olivine are not expected to exhibit an anomalous curvature at pressures of the mantle transition zone.

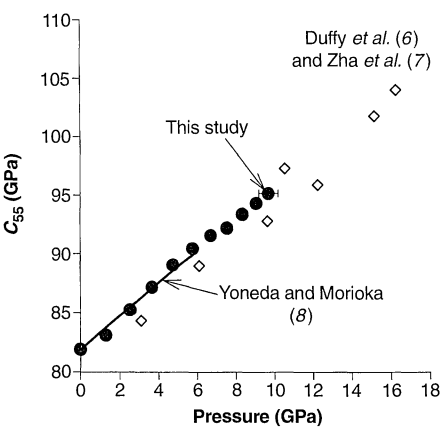

Fig. 2. Shear elastic modulus C_{55} versus pressure for single crystals of synthetic forsterite (Mg_2SiO_4). Filled circles, data from this study; diamonds, data from (*6, 7*); and solid line, data from (*8*). Uncertainties are as in Fig. 1.

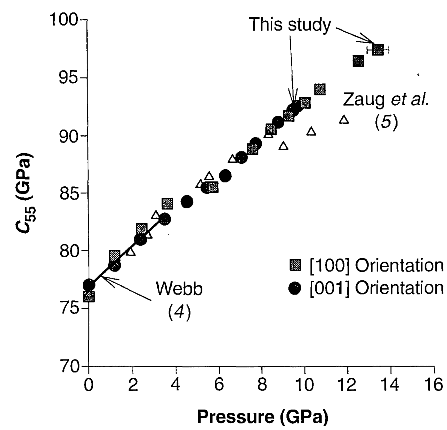

Fig. 3. Shear elastic modulus C_{55} versus pressure for San Carlos olivine. Filled circles and filled squares, data from this study; solid line, data from (*4*); and triangles, data from (*5*). Uncertainties are as in Fig. 1. Error bars of (*5*) are about the size of the symbols.

Table 1. Summary of C_{55} data for olivine and forsterite as a function of pressure.

Source	C_{55} ambient (GPa)	$\partial C_{55}/\partial P$	Comment
	Natural San Carlos olivine [$(Mg_{0.9}Fe_{0.1})_2SiO_4$]		
This study	77.2	1.56	To >12 GPa
Webb (*4*)	76.9	1.62	Refit her data with straight line (measurements to 3 GPa)
Zaug *et al.* (*5*)	77.0	2.18	$\partial^2 C_{55}/\partial P^2 = -0.16$/GPa (*11*)
Kumazawa and Anderson (*1*)	76.9	1.80	To 0.2 GPa
	Synthetic pure forsterite (Mg_2SiO_4)		
This study	81.9	1.41	To ~10 GPa
Duffy *et al.* (*6*) and Zha *et al.* (*7*)		1.38	To 16 GPa
Yoneda and Morioka (*8*)	81.2	1.40	Refit their data with straight line (measurements to 6 GPa)
Bassett *et al.* (*12*)	83.8	1.50	To 4 GPa
Graham and Barsch (*2*)	81.4	1.65	To 1 GPa
Kumazawa and Anderson (*1*)	78.1	1.64	To 0.2 GPa

REFERENCES AND NOTES

1. M. Kumazawa and O. L. Anderson, *J. Geophys. Res.* **74**, 5961 (1969).
2. E. K. Graham and G. R. Barsch, *ibid.*, p. 5949.
3. T. S. Duffy and D. L. Anderson, *ibid.* **94**, 1895 (1989).
4. S. L. Webb, *Phys. Chem. Minerals* **16**, 684 (1989).
5. J. M. Zaug *et al.*, *Science* **260**, 1487 (1993).
6. C. S. Duffy *et al.*, *Nature* **378**, 170 (1995).
7. C. S. Zha *et al.*, *J. Geophys. Res.*, in press.
8. A. Yoneda and M. Morioka, in *High-Pressure Research: Application to Earth and Planetary Sciences*, Y. Syono and M. H. Manghnani, Eds. (American Geophysical Union, Washington, DC, 1992), pp. 207–214.
9. B. Li *et al.*, in preparation. For the ultrasonic measurements in the multi-anvil apparatus, the sample is surrounded by lead on the sides. On the bottom, it is backed by a Teflon disk (to enhance acoustic impedance mismatch) and then again by lead. The lead provides a pseudohydrostatic pressure environment and protects the sample from cracking at high pressures. Optical and transmission electron microscope (TEM) examination of the recovered sample after an experiment to a pressure $P > 10$ GPa revealed no cracks and no increase in the dislocation density, thereby demonstrating the absence of any significant deviatoric stress. To prevent the lead from extruding to the gasket area between the cubes while applying pressure, we inserted the sample and the surrounding lead into a steel sleeve. Bismuth and ZnTe, which were embedded in the Teflon disk backing the sample, served as in situ pressure markers because the change in their resistance with pressure could be monitored. Therefore, the pressure scale in each individual run could be obtained from the observed phase transformations in Bi (I to II, 2.55 GPa; III to V, 7.7 GPa) [M. Nomura *et al.*, *Jpn. J. Appl. Phys.* **21**, 936 (1982); E. C. Lloyd, *Natl. Bur. Standards Spec. Publ.* **326** (1971), pp. 1–3] and ZnTe (I, 9.6 GPa; II, 12.0 GPa) [K. Kusaba *et al.*, *Pure Appl. Geophys.* (Schreiber Memorial Volume, R. C. Liebermann and C. H. Sondergeld, Eds.) **141**, 644 (1993)]. The reproducibility of the cell pressure is better than 1% for the same ram force, and the pressure gradient is about 0.25 GPa/mm across the sample.
10. Single-crystal samples of San Carlos olivine and forsterite were oriented with the x-ray diffraction method to better than 1°. The forsterite sample was cut off from one of the specimens used by Yoneda and Morioka (*8*). The geometry of the sample is a solid cylinder polished to optical quality at both ends, with a diameter of 2 to 3 mm and a length of 1 to 2 mm. A piezoelectric transducer (40-MHz $LiNbO_3$) was bonded to a truncated, stress-free corner of one of the tungsten carbide cubes, which served as an acoustic buffer rod and in addition transmitted pressure to the cell assembly. The sample was coupled to the buffer rod with a 2-μm gold foil.
11. Quadratic fit of C_{55} versus pressure by T. S. Duffy is based on the data in figure 1 of Zaug *et al.* (*5*).
12. W. A. Basset *et al.*, in *High-Pressure Research in Geophysics*, S. Akimoto and M. H. Manghnani, Eds. (Center for Academic Publications, Tokyo, 1982), pp. 115–124.

13. We thank A. Yoneda for supplying the forsterite samples. We thank J. Ando who performed the TEM study on one of the recovered olivine samples to examine the dislocation density and helped to orient the San Carlos olivine samples. We thank T. Duffy and C. Zha who shared data on forsterite with us. Discussions with D. J. Weidner and Y. Wang led to improvements in this report. These high-pressure experiments were conducted in the Stony Brook High Pressure Laboratory, which is jointly supported by the State University of New York at Stony Brook and the NSF Science and Technology Center for High Pressure Research (EAR-89-20239). This research was also supported by EAR-93-04502. Mineral Physics Institute contribution 171.

20 December 1995; accepted 27 March 1996